AIP | Journal of Applied Physics

The investigation of point defect modes of phononic crystal for high Q resonance

Feng Li, Jun Liu, and Yihui Wu

Citation: J. Appl. Phys. **109**, 124907 (2011); doi: 10.1063/1.3599866
View online: http://dx.doi.org/10.1063/1.3599866
View Table of Contents: http://jap.aip.org/resource/1/JAPIAU/v109/i12
Published by the American Institute of Physics.

The investigation of point defect modes of phononic crystal for high Q resonance

Feng Li,[1] Jun Liu,[1,2] and Yihui Wu[1,a)]
[1]*State Key Laboratory of Applied Optics, Changchun Institute of Optics, Fine Mechanics and Physics, Chinese Academy of Sciences, Changchun 130022, China*
[2]*Graduate School of Chinese Academy of Sciences, Beijing, China*

(Received 30 November 2010; accepted 12 May 2011; published online 24 June 2011)

Point defect cavity was constructed in a two-dimensional phononic crystal plate. It was excited by a small piezo chip in the cavity, and the vibrations of each point defect mode were detected by an optical interferometer. Point defect modes on 2D phononic crystal plate in vacuum, air, and with water loaded were investigated theoretically and experimentally. It is shown that the Q factors of the point defect modes are determined by inner attenuation, bandgap effects, and medium. The SSS mode (breathing mode) has highest Q factor in vacuum and air among nine modes thanks to low inner attenuation and low energy leakage. By selectively loading the PC with water on one side, the point defect modes with shear movement surfaces suffer lower attenuation and still have rather high Q factors. These conclusions will help to design a new kind of resonator or sensor. © *2011 American Institute of Physics*. [doi:10.1063/1.3599866]

I. INTRODUCTION

Recent studies have shown that the localized modes can be obtained by putting defects in phononic crystals (PC) and making their resonate frequencies within the bandgap.[1–3] These are attractive to get high Q and mode tuning resonators or sensors. Mohammadi got high Q factor linear defect modes in a 2D PC plate.[4] In fact, it is not hard to call to mind that point defect mode in PC could have better energy confinement than linear defect mode.[5] The experimental studies about point defect mode on PC, especially the interactions between defect mode and medium, are rare. The defect modes are often studied by transmission spectrum, which results in low signal due to the exponential attenuation of the bandgap, especially when the size is limited and the number of PC layers is large. Furthermore, there are often several modes in the defect cavity of PC, and it is important to understand the behavior of the defect modes within the bandgap.

In this paper, point defect cavity was constructed in a two-dimensional phononic crystal plate because 2D PC plate is easier to fabricate comparing with 3D PC. It was excited by a small piezo chip inside the cavity, and the vibrations of each point defect mode were detected by an optical interferometer directly, thus the wave propagation in PC is avoided. Point defect modes on 2D PC plate in vacuum, air, and loaded with water were investigated theoretically and experimentally in order to know the influences of the inner attenuation, the bandgap effects, and the medium.

II. SETUP OF EXPERIMENTS AND CALCULATION

The setup of the experimental system is shown in Fig. 1. A matrix of 500 holes (Φ 4.00 mm) were drilled through a steel circular plate (4.54 mm thick) to form a honeycomb lattice PC. The defect cavity was created by filling two proximate holes in the center of PC. The Ra roughness of the plate and the holes are 1.6 μm and 6.3 μm respectively. The position error of the holes is about 10 μm. The density, the Young's modulus, and the Poisson ratio of the steel were 7750 kg/mm^3, 206 GPa, and 0.28, respectively. A small piezo rectangular chip of $1.5 \times 1.5 \times 0.2$ mm^3 was sandwiched by metal film and the steel plate. The electrode was fixed on the cavity as shown in Fig. 1, and 15 dBm source power from network analyzer (Agilent 4395 A) was adopted. The laser beam from the interferometer was focused and scanned through the surface of the defect cavity. In this way, the vibrations of defect cavity were obtained by the optical interferometer without wave propagations in PC. The output of the interferometer was connected to the analyzer. By sweeping the exciting frequency, 2D amplitude and phase plots versus position and frequency can be obtained.

The simulation of the PC devices was carried out by the 7×7 supercell method using finite element method (FEM).[6] The honeycomb lattice PC plate provided a wide bandgap from 208.2 kHz to 292.6 kHz. There are nine point defect modes located in the bandgap. These modes can be classified according to the symmetry of the point defect cavity, which is similar to microwaves in a waveguide.[7] In our case, the defect modes were classified as 8 types considering the anti-symmetry or symmetry with respect to YOZ, XOZ, or XOY planes. For example, SSA mode is symmetric with respect to YOZ and XOZ planes; it is anti-symmetric with respect to XOY plane. The two AAS modes were distinguished as AAS0 and AAS1 modes. The deformation patterns of these modes are shown in Fig. 2, and the displacements in Z direction are plotted in color scale.

III. RESULTS AND DISCUSSIONS

A. Amplitudes and phases of point defect modes

Because the optical interferometer is only sensitive to the vibration in Z direction, the amplitudes in Z direction

a)Author to whom correspondence should be addressed. Electronic mail: yihuiwu@ciomp.ac.cn.

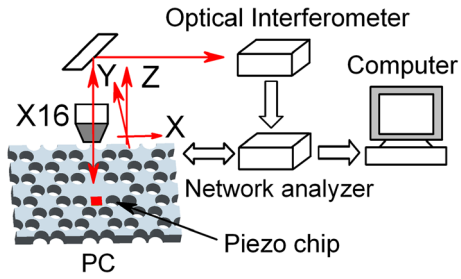

FIG. 1. (Color online) The model of the point defect cavity on the PC and the measurement setup.

and the phases of the point defect cavity vibration in X and Y axes were measured by the optical interferometer. The amplitudes in Z direction and phases at given position or frequency are represented in Fig. 3. At a resonant frequency, the nodes and the antinodes of the defect modes are clearly shown. There are 180° phase shifts at all nodes; these mean the vibration directions of neighbor antinodes are opposite and all defect modes act as standing wave in both X and Y directions. All the simulated modes in Fig. 2 are observed experimentally in Fig. 3. The measurements agree with calculation well and the relative frequency deviations between measurement and simulation are, on average, less than 2%.

B. Q factors of point defect modes in vacuum

From 3 dB bandwidth of amplitude responses in Fig. 3, the experimental Q factors of each defect mode can be obtained. There are several factors contributing to Q factor, which can be approximately explained by[8]

$$\frac{1}{Q}=\frac{1}{Q_m}+\frac{1}{Q_{pc}}+\frac{1}{Q_{air}}. \quad (1)$$

$1/Q_m$ corresponds to ultrasonic attenuation of the metal, $1/Q_{pc}$ corresponds to bandgap leakage, and $1/Q_{air}$ is attenuation due to air. By putting the PC into a vacuum chamber and measuring the amplitude response in vacuum (less than 1 mbar), the effect of air on defect modes can be avoided.

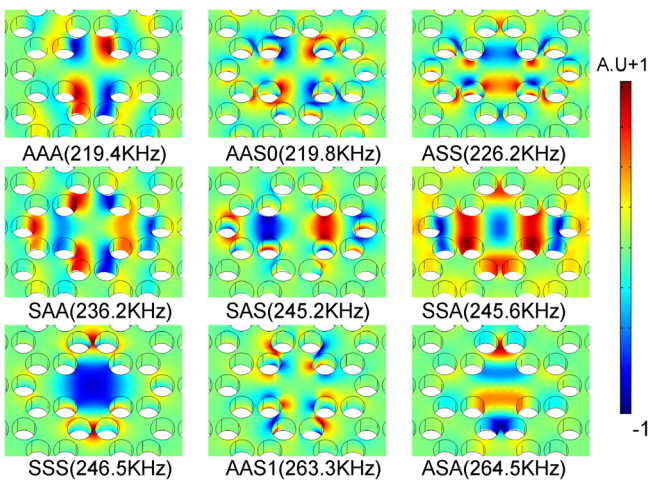

FIG. 2. (Color online) The eigen point defect modes pattern (the color bar corresponds to the displacement in Z direction) from FEM calculation. The modes were classified according to the symmetry of the point defect cavity.

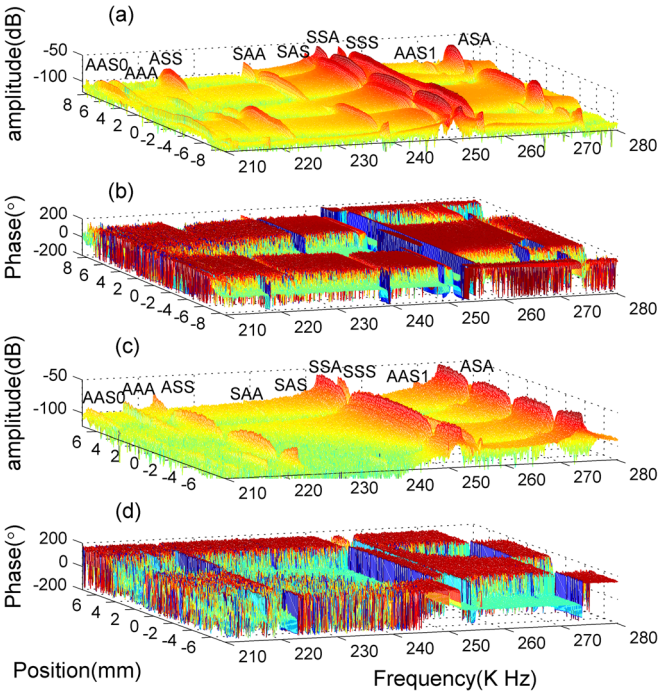

FIG. 3. (Color online) The amplitude and phase of the point defect cavity at given position or frequency. (a) is the amplitude variations along X axis, (b) is the phase variations along X axis, (c) is the amplitude variations along Y axis, (d) is the phase variations along Y axis.

The Q factors of defect modes in vacuum and the measurement errors are shown in Fig. 4, respectively. In this situation, the difference of Q factors of each mode probably come from the material attenuation and the energy leakage of the PC. The Q factor of AAA mode is the lowest among the nine modes, while SSS mode (so called breathing mode) is the highest one and reached 3.2×10^4.

The ultrasonic attenuation of the metal was due to hysteretic attenuation and Rayleigh scattering due to metal grain. Since shear movement suffers more scattering than longitude movement,[9] ultrasonic attenuation of shear wave is larger than that of longitude wave. In our case, the material attenuation of the complex movement can be analyzed by decomposing the modes into compressive movement and shear movement. Q_m in Eq. (1) of each mode can be compared by

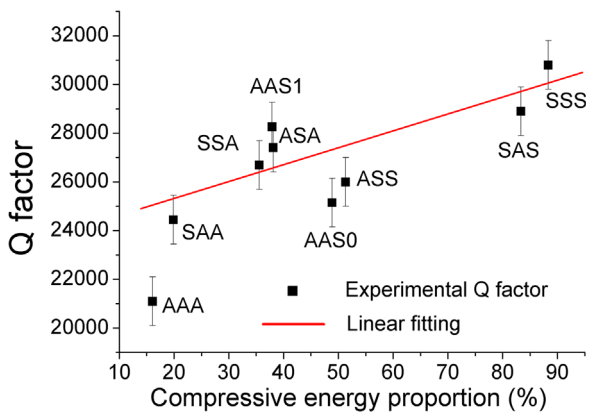

FIG. 4. (Color online) The relationships between Q factors of the point defect mode and the compressive energy percentages of each mode.

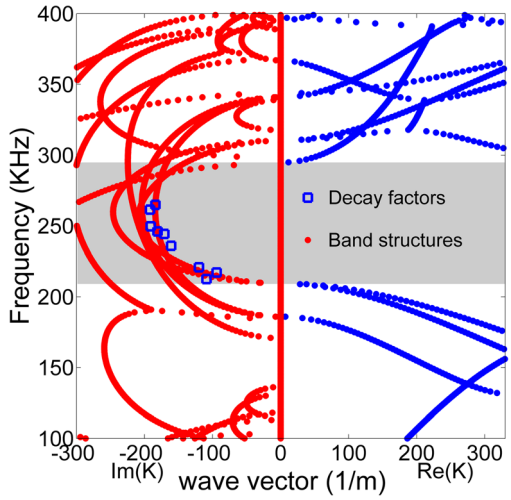

FIG. 5. (Color online) The complex band structure for complete PC (dot) in ΓX direction. Im(K) is the imaginary part of wave vectors and Re(K) is the real part of wave vectors. By numerically fitting the point defect modes' amplitude, the decay factors of nine point defect modes were obtained and shown in square.

calculating the compressive energy percentage of each mode. The compressive energy percentages of all modes were obtained by summing up compressive energy of each element of the supper cell. The relationship between measured Q factors in vacuum and compressive energy percentages are represented in Fig. 4. It is shown that the Q factors increase with compressive energy proportion: AAA mode has the lowest compressive energy proportion (16%) and the lowest Q factor, while the SSS mode is mainly in compressive movement (88%) and has the highest Q factor.

In Fig. 4, the Q factors of the first three modes are lower than linear fitting. The disagreement of the first three modes in Fig. 4 can be explained by bandgap leakage, which is determined by the imaginary part of complex band structure. We obtained the complex band structure of perfect PC by applying supercell method to plane wave expansion (PWE) and using k(ω) method.[10,11]

In the PWE calculation model, the supercell plate is sandwiched by low impedance medium (LIM) on both sides. The LIM layers are ten times the thickness of plate and $9 \times 9 \times 7$ reciprocal lattice vectors are used in the calculation. The imaginary and real band structures in ΓX direction for the complete PC are represented in Fig. 5. The gray region between 208.2 kHz and 292.6 kHz shows the bandgap of PC. Im(k) and Re(k) are the imaginary and real part of wave vectors. Their imaginary curves (left side of Fig. 5) correspond to the decay factors of evanescent waves and depend both on frequency and wave pattern. In Fig. 5, the decay factors in the center bandgap may be higher than that at the edge of the bandgap. The decay factors of the defect modes in Y direction can be obtained by numerically fitting the amplitude of FEM results with exponential function ae^{-bx}. The numerical fitting decay factors of the nine point defect modes (in square) were also shown in Fig. 5. The decay factor b of AAS1 mode is -192 m^{-1}, which is much higher than that of AAA (109 m^{-1}), thus AAS1 mode has better localization then AAA mode. This explains why the Q factors of the first three modes are lower than the expected values.

C. Q factors of point defect modes in air and loaded with water

When the air was introduced into vacuum chamber, all of the Q factors decreased due to the air damping which is shown in Fig. 6. The acoustic radiation is mainly due to the normal displacement of the cavity at the interface between air and PC.[12] The square normal velocity over the total structure normalized by total energy can be obtained from Fig. 2 and are represented in Fig. 7. SSS mode (the breathing mode) has the lowest square normal velocity, thus it suffers lowest damping and still has the highest Q factors in air. It also explains why the third mode suffers large air damping.

Contrary to the weak disturbance by air to the PC, the bandgap will close and the defect modes will disappear if the PC is immersed in the liquid completely, due to the strong coupling between PC and liquid. However, if the liquid was selectively loaded on part of the PC, some of the defect mode may still exist. In our case, the interaction between liquid and defect mode was investigated by keeping all the holes empty and loading liquid only on one side of the PC; this is also the general way when acoustic devices work for

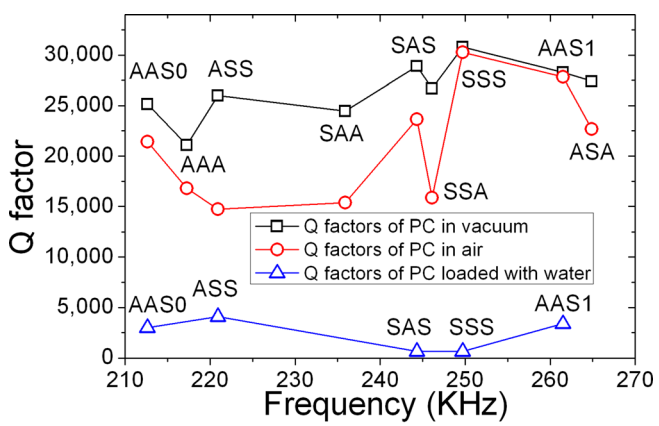

FIG. 6. (Color online) The Q factors of the point defect mode of PC in vacuum, air, and loaded with water on one side.

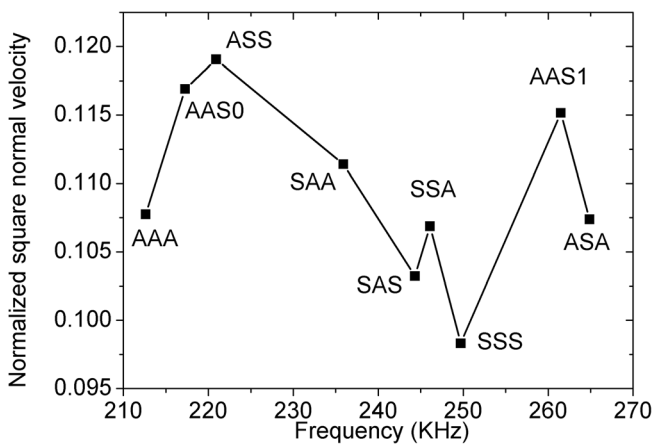

FIG. 7. The calculated normalized square normal velocity of the point defect modes.

liquid detection, such as Love wave and Lamb wave sensors.[13]

With water loading in our experiments, the resonance of AAA, SAA, SSA, and ASA mode disappeared, while AAS0, ASS, SAS, SSS, and AAS1 modes still exist, and their Q factors are represented in Fig. 6. The Q factors of all modes decreased because of the liquid damping. The XOY symmetric modes with shear movement between plate and water surfaces suffer less attenuation. The ASS mode vibration is almost tangential to the plate and water interface; the wave barely penetrates the liquid and its Q factor reached 4000. Although SSS mode has highest Q factor in vacuum and air, it dilates normal to the plate and water interface and suffers more attenuation than ASS mode.

IV. CONCLUSIONS

In conclusion, acoustic energy can be confined efficiently by PC, which was shown by optical interference measurement. The signal wave propagation from the cavity to the outside is avoided by exciting and measuring the defect cavity inside. We found that the Q factors of PC in vacuum are mainly determined by inner attenuations and are affected by imaginary decay factors. As an example, SSS (breathing) mode has highest Q factor in vacuum among nine modes due to low inner attenuation and low energy leakage. The Q factors of all modes decrease due to air damping, while SSS mode is less sensitive to air thanks to less square normal velocity over the total structure. By selectively loading the PC with water on one side, the interactions between liquid and high Q defect cavity were studied. Even though all the modes suffer strong liquid damping, the XOY symmetric point defect modes suffer lower attenuation and still have rather high Q factors. These conclusions are significant for design and optimization of high Q defect mode resonator or sensor.

ACKNOWLEDGMENTS

The work was founded by the Natural Science Foundation of China (60871043, 60971025, and 11034007) and the Key Knowledge Innovation Project of The Chinese Academy of Sciences (KJCX2-YW-H18).

[1]M. Torres, F. R. Montero de Espinoza, D. Garcia-Pablos, and N. Garcia, Phys. Rev. Lett. **82**, 3054 (1999).
[2]I. E. Psarobas, N. Stefanou, and A. Modinos, Phys. Rev. B **62**, 5536 (2000).
[3]X. Li and Z. Y. Liu, Phys. Lett. A **338**, 413 (2005).
[4]S. Mohammadi, A. A. Eftekhar, W. D. Hunt, and A. Adibi, Appl. Phys. Lett. **94**, 051906 (2009).
[5]H. Zhong, F. G. Wu, X. Zhang, and Y. Y. Liu, Phys. Lett. A **339**, 478 (2005).
[6]J. O. Vasseur, P. A. Deymier, B. Jafrri-Rouhani, Y. Pennec, and A-C. Hladky-Hennion, Phys. Rev. B **77**, 085415 (2008).
[7]P. R. McIsaac, IEEE Trans. Microwave Theory Tech. **23**, 421 (1975).
[8]K. Y. Yasumura, T. D. Stowe, E. M. Chow, T. Pfafman, T. W. Kenny, B. C. Stipe, and D. Rugar, J. Microelectromech. Syst. **9**, 117 (2000).
[9]E. P. Papadakis, J. Appl. Phys. **35**, 1474 (1964).
[10]V. Laude, Y. Achaoui, S. Benchabane, and A. Khelif, Phys. Rev. B **80**, 092301(2009).
[11]J. O. Vasseur, P. A. Deymier, B. Djafari-Rouhani, Y. Pennec, and A.-C. Hladky-Hennion, Phys. Rev. B **77**, 085415 (2008).
[12]F. J. Fahy and P. Gardonio, *Sound and Structural Vibration: Radiation, Transmission and Response*, 2nd ed. (Elsevier, New York, 2007).
[13]B. Drafts, IEEE Trans. Microwave Theory Tech. **49**, 795 (2001).